PCCP

Accepted Manuscript

ROYAL SOCIETY OF CHEMISTRY

www.rsc.org/pccp

Excited State Proton Transfer Dynamics of an Eminent Anticancer Drug, Ellipticine in Octyl Glucoside Micelle

Krishna Gavvala, Raj Kumar Koninti, Abhigyan Sengupta, Partha Hazra*

Department of Chemistry, Indian Institute of Science Education and Research (IISER), Pune-411008, Maharashtra, India.

* Corresponding author. E-mail: p.hazra@iiserpune.ac.in. Tel.: +91-20-2590-8077; Fax: +91-20-2589 9790.

Abstract

Photophysics and proton transfer dynamics of an eminent anticancer drug, ellipticine (EPT) have been investigated inside a biocompatible octyl-β-D-glucoside (OBG) micellar medium using steady state and time-resolved fluorescence spectroscopic techniques. EPT exists as protonated form in aqueous solution of pH 7. When EPT molecules are encapsulated in OBG micelles, protonated form is converted to neutral form in the ground state due to the hydrophobic effect of the micellar environment. Interestingly, steady state fluorescence results indicate the existence of both neutral and protonated forms of EPT in the excited state, even though neutral molecules are selectively excited, and it is attributing to the conversion of protonated to neutral form of EPT by excited state proton transfer (ESPT) process. A clear isoemissive point in the time-resolved area normalized emission spectra (TRANES) further supports the excited state conversion of neutral to protonated form of EPT. Notably, this kind of proton transfer dynamics is not observed in other conventional micelles, such as, SDS, Triton-X and CTAB. Therefore, the observed ESPT dynamics is believed to be an outcome of combined effects of local dielectric constant felt by EPT and local proton concentration at the OBG micellar surface.

Keywords: Anticancer drug, octyl-β-D-glucoside, micelles, ESPT, TRANES.

Introduction

Alkyl glucosides are the class of non-ionic surfactants, widely used in food, cosmetic and pharmacy products. Alkyl glucosides contain a hydrophilic part comprised of glucose moiety, and a hydrophobic part consisting of hydrocarbon chain. These sugar surfactants are non-toxic and can be synthesized from renewable resources.[1,2] Another important aspect of these surfactants is their biodegradable nature. The main reason for the biodegradability is the presence of glucoside linkage, which widely occurs in nature, and its formation and breakage are controlled by different glucosidases.[3] These properties make them perfect substitutes of other surfactants, which are potentially dangerous to the environment. These biocompatible OBG surfactants are frequently used to study the dissolution and formation of biological membranes as well as the stabilization of proteins.[4-8] Considering the bio-compatible behavior of the alkyl glucoside, the micellar aggregate of these sugar based surfactants may be used as potential drug delivery carrier. It is important to understand the effect of the micellar confinement on solubility and stability of drug in order to use it in pharmaceutical field. Moreover, the dynamics study of drug molecules inside the glucoside micelle is very essential in order to get insight into the effect of confined environment on the stability of the drug molecules. In the present study, we have studied the modulation of proton transfer dynamics of a well known anticancer drug, ellipticine, when it is encapsulated inside one of the well studied glucoside micelle, namely, octyl-β-D-glucoside (OBG) micelle. We have chosen octyl-β-D-glucoside (OBG) because many properties such as phase diagram, structural behavior of the OBG have been extensively studied by various techniques.[9-21]

Ellipticine (5,11-dimethyl-6H-pyrido[4,3-b]carbazole), a pyridocarbazole alkaloid, a potential anticancer drug, was first isolated from the leaves of *Ochrosia elliptica* by Goodwin et al. in 1959.[22] Ellipticine (EPT) intercalates in DNA and inhibits the activity of DNA topoisomerase-II, which results inhibition of DNA replication and transcription process of

RNA.[23-25] Due to the presence of basic pyridine nitrogen,[26] EPT exists in two prototropic forms depending on the pH as well as environmental polarity (Scheme 1). It was found that EPT exists as neutral form in non-polar and hydrophobic media, and exhibits emission peak in the range of 410-440 nm.[27] Ellipticine exists as protonated form in hydrophilic medium and emits at ~530 nm; whereas in methanol and ethylene glycol the drug exhibits concomitant dual emission at ~430 nm and ~510 nm.[27-29] Miskolczy *et al.* assigned the red edge emission of EPT to excited state proton transfer reaction by the solvent.[28] Recently, Samanta and coworkers reported solvent mediated excited state intramolecular proton transfer from the pyrrole nitrogen to pyridine nitrogen as origin of fluorescence from protonated EPT.[29]

Previous studies have revealed that ellipticine exists as neutral form in cell cytoplasm and protonated form at nucleus.[26] Although ellipticine is considered as a potential anti-tumor drug, the major disadvantages in the usage of ellipticine in pharmaceutics are its toxicity and low solubility in aqueous solution. It is a big challenge for the researchers to improve the solubility and targeted delivery of the drug using biocompatible drug carriers. To understand how ellipticine is transported to its target, it is very important to establish a relationship between the environment and the photophysical properties of EPT. For that purpose the photophysical properties of the drug have been investigated in several confined and self-assembled systems such as cyclodextrins, cucurbiturils, micelles, reverse micelles, vesicles, bile salts and polymers.[30-35] Although several attempts have been made on photophysical properties of the drug in many biological and biomimicking media, to date excited state proton transfer dynamics of EPT has seldom been monitored in the aforementioned confined environments. Herein, we report the encapsulation of EPT drug in OBG micelles and the consequences of confinement on photophysical properties of EPT using steady state and time-resolved spectroscopic techniques. The focus of this work is to understand the effect of

confinement on proton transfer dynamics of ellipticine. Interestingly, we have observed that proton transfer is dramatically slowed down when the drug molecules are encapsulated in OBG micelles, which resulted emission from both the neutral and protonated forms of EPT. We have also constructed time resolved emission spectrum (TRES) and time resolved area normalized emission spectrum (TRANES), which provides information about the existence of multiple emissive species in the excited state. Finally, these results are compared with other conventional micelles such as CTAB, SDS and Triton-X, and we have observed that any such excited state proton transfer process is absent in the above mentioned three micelles.

Experimental

Ellipticine (EPT), octyl-β-D-glucopyranoside (OBG), glucose, sodium dodecyl sulfate (SDS), cetyltrimethylammonium bromide (CTAB) and Triton X-100 were purchased from Sigma Aldrich, and used without further purification. All the samples were prepared in phosphate buffer (10 mM), unless otherwise mentioned. Concentration of EPT in water was adjusted to ~10^{-5} M using reported value of molar extinction coefficient (ε_{300} = 39000 M^{-1} cm^{-1}).[36]

Absorbance measurements were performed on Perkin-Elmer UV-visible spectrophotometer (Lambda-45), and steady-state fluorescence spectra were recorded on FluoroMax-4 spectrofluorimeter (Horiba Scientific, USA). All time-resolved fluorescence measurements (both lifetime as well as anisotropy) were performed on a time correlated single photon counting (TCSPC) spectrometer (Horiba Jobin Yvon IBH, U.K.). The detail description of the instrument is described elsewhere.[37,38] Here, we have used 375 nm diode laser for exciting drug molecules. The analysis of emission decays was done by IBH DAS6 analysis software. We have fitted both lifetime data with a minimum number of exponential. Quality of each fitting was judged by χ^2 values and the visual inspection of the residuals. The value of χ^2 ≈1 was considered as best fit for the decays.

Results and Discussion

Steady state measurements: Absorption spectra of EPT in buffer and in presence of OBG are shown in Figure 1a. The drug in buffer exhibits several peaks in 250-450 nm region with a peak maximum at 300 nm and two shoulders at 350 nm and 420 nm. Earlier reports divulge that these are the characteristic peaks of protonated form of EPT.[26] On gradual addition of OBG, absorption profile of EPT does not change significantly until certain concentration (≤ 25 mM). At higher concentration of OBG (≥ 26 mM), noteworthy changes are observed in absorption spectra (Figure 1a). The peaks representing protonated form (300 nm and 425 nm) are almost vanished and two new peaks are appeared at ~280 nm and ~380 nm. These new peaks were previously observed in many instances, when EPT was incorporated in hydrophobic media.[35,39,40] Therefore, the above observations infer that EPT experiences hydrophobic environment above certain concentration of OBG (26 mM) and thereby, ground state neutral form generates at the cost of protonated form of EPT. Interestingly, the concentration of OBG (≥26 mM) after which the changes in absorption spectra of EPT observed is in good agreement with the previously reported critical micellar concentration (CMC) of OBG.[41]

Emission profiles of EPT in phosphate buffer and in presence of OBG are shown in Figure 1b. EPT exhibits single emission maximum at 530 nm, which is believed to be originated from protonated form of the drug.[26] With the gradual addition of OBG to the buffer containing EPT solution, the fluorescence intensity at 530 nm slightly increases along with a small hump in the 420-450 nm region. However, at concentration ≥26 mM, the 530 nm peak shoots up with a prominent new peak at 440 nm (Figure 1b). The 440 nm peak also grows up and becomes comparable to the 530 nm peak at higher concentration of OBG. This kind of fluorescence switch of EPT from 530 nm in buffer to 440 nm in micelles is unique and can be visualized directly from the color change of solution from green to cyan (Figure

S1). It is already well established that EPT residing in hydrophobic environment emits the blue region (420-440 nm),[30,39,40] and it is believed to be appeared from the neutral form of the drug. Thus, we believe that the newly appeared peak at 440 nm is coming from the neutral drug molecules. Hence, the appearance of blue emission at 440 nm demonstrates that conversion of the drug takes place from protonated to neutral form in presence of OBG micellar environment. However, if this switching of the form would be the case for the increment of neutral form peak intensity, then the intensity at 440 nm, which is signature peak of neutral form of EPT, should have been increased at the cost of protonated form peak intensity at 530 nm. Astonishingly, the intensity at 530 nm concomitantly increases along with 440 nm peak with the gradual hike in OBG concentration. Here it is necessary to mention that absorption results confirmed that transformation takes place from protonated to neutral form in OBG micelle (Figure 1a). Moreover, the excitation spectra monitored at 440 nm and 530 nm are very similar (Figure S2, Note S1). Based on above observations, we envisage that although in the ground state the population of neutral form of the drug increases in the micellar environment (probably due to decrease surrounding polarity of the drug), in the excited state some of the neutral form of drug molecules are converted to the protonated form by excited state proton transfer process. As a result, the intensity of both the neutral as well as protonated form increases with OBG concentration.

The above results indicate that drug molecules are not buried completely inside the hydrophobic domain of the micelle, as protonated species in the excited state is not at all stable in the hydrophobic domain of the micelle. We guess the drug molecules reside near the palisade layer of the micelle, where hydrophilic sugar head groups of the surfactant are present. In order to confirm the effect of glucose moieties present in the micelle, the drug fluorescence was monitored with increasing concentration of glucose. Neither intensity enhancement nor new peak appearance was observed in emission spectrum of EPT up to 500

mM of glucose (Figure S3) and it suggests that presence of sugar moieties are not solely responsible for the observed photophysics of the EPT. To verify the effect of confined environment of the micelle, we have also collected the emission spectra of EPT in three different types of micelles, namely cationic, anionic and neutral micelles and the observed results are in good agreement with the literature reports.[31] In case of anionic SDS micelles, EPT exhibits protonated peak at 530 nm, whereas it shows peak at ~440 nm in CTAB micelle (Figure S4). Notably, although TX-100 surfactant head group contains –OH group, the micellar environment of TX-100 does not exhibit any protonated peak of ellipticine at 530 nm (Figure S4). Therefore, the appearance of both the peaks in case of OBG micelles is believed to be an outcome of confined as well as polarity of the surrounding environments. Although we have proposed that excited state proton transfer is the origin of green emission in OBG micellar environment, in order to gain deeper insight into the excited state proton transfer process we have performed time resolved measurements, which is discussed in the next section.

Time-resolved measurements: Time-resolved fluorescence measurement is an excellent technique to monitor the excited state dynamics of molecules and is a unique method to identify multiple emissive species present in a given system.[42] Emission decay profiles of EPT in absence and in presence of OBG are collected at 440 nm and 530 nm in order to monitor the excited state dynamics of both neutral and protonated species, respectively (Figure 2). As shown in Table 1, protonated EPT (at 530 nm) exhibits bi-exponential decay profile in buffer having individual lifetime components of ~2 ns (87%) and ~6 ns (13%) with an average lifetime value of ~2.5 ns. In the present scenario, the assignment of individual component is complicated, as our lifetime profile consists of only decaying components. In case of methanol, where people observed dual emission, the decay profile at longer wavelength consists of a growth followed by decaying component. Moreover, the

growth component lifetime was exactly matching with the decaying component of shorter wavelength. Therefore, it was easy to predict that the growth component to the excited state proton transfer process. As our decay profile in buffer is devoid of any growth component, it is difficult to assign individual components.

With the successive addition of OBG, the average fluorescence lifetime of EPT collected at 530 nm steadily increases until 26 mM of OBG. After 26 mM of OBG, the average lifetime shoots up to ~20 ns (Figure 2 and Table 1). The increased average lifetime infers that the stability of protonated EPT is enhanced in presence of OBG micellar environment, as it is evident that OBG forms micellar assembly after 26 mM. The most intriguing observation is the appearance of ~4 ns growth component after 26 mM of OBG (τ_3 in Table 1a). Moreover, the contribution of growth component increases with OBG concentration. Notably, this kind of long growth component of EPT was not observed in other confined environments, like reverse micelle, lipid bilayers, cyclodextrin/cucurbituril nano-cavity etc., and in that sense the growth feature observed in lifetime profile is unique. There are two possibilities for the appearance of growth component in the fluorescence transient; either due to the slow solvation dynamics or due to the excited state reaction, such as proton transfer process. In order to verify the first possibility, we have collected emission transients at longer wavelengths (red edge side) and the results depict no significant change in the growth component. This finding confirms the growth component appeared in the decay profile is not because of solvation, but may be due to the excited state proton transfer process. To unveil the proton transfer mechanism, we have further collected fluorescence transients at 440 nm, which is believed to be originated from neutral form of the drug. In buffer medium, EPT exhibits tri-exponential decay at 440 nm with individual lifetime components of ~40 ps, ~290 ps and ~2.3 ns exhibiting an average lifetime of ~160 ps. It is evident from Figure 1b

that the intensity of EPT at 440 nm is negligibly small in buffer medium. Moreover, protonated EPT also contributes significantly towards the intensity at 440 nm, and therefore, we believe the decay feature observed at 440 nm cannot be attributed solely to the neutral EPT molecules. However, we have collected the decay profile even at 440 nm in order to compare the dynamics of neutral EPT molecules generated in presence of OBG micellar environment. It is clear from the lifetime results that the average lifetime collected at 440 nm, which is believed to be originated from neutral drug, steadily increases with addition of OBG and jumps up to ~4 ns at ≥26 mM of OBG (CMC of OBG micelle). It is interesting to notice that the growth component (~4 ns) observed at 530 nm is in good agreement with one of the lifetime components collected at 440 nm (Table 1b). This confirms that protonated form generates at the cost of neutral form, and the conversion of neutral to protonated form takes place through excited state proton transfer process. To confirm the presence of two different types of species in the excited state, we have further constructed time resolved area normalized emission spectrum (TRANES), a recently developed technique to explore excited state components. TRANES method is a one-step extension of the commonly used time resolved emission spectrum (TRES) analysis.[43,44] TRES and TRANES of EPT between time 0.1 and 30 ns in presence of OBG micelles are shown in Figure 3. A clear isoemissive point at 480 nm is noticeable in TRANES, indicating that the existence of equilibrium between neutral and protonated forms of the drug in the excited state. It is clear from TRANES that initial population is dominated by neutral species, however, at sufficiently longer time-scale the protonated species becomes dominated compared to the neutral one. This further supports our conjecture that protonated species generate at the cost of neutral one in the excited state. It is already discussed that the lifetime of protonated species consists of growth component (~4 ns), which is believed to be the formation time-scale of protonated form. In TRANES, we have also noticed that the reasonable intensity of protonated form is appearing after 4 ns.

Therefore, these results confirm that proton transfer process takes place in OBG micelle in ~4 ns time scale. Earlier reports also elucidate that proton transfer dynamics can be slower in constrained environments.[45-49] No isoemissive point is observed below CMC of OBG micelle and in presence of glucose alone. Moreover, this kind of ESPT process is totally absent in other micelles, like SDS, CTAB and TX-100 micelles (Figure S5, Note S2). Therefore, based on the above observations, we anticipate that OBG micelle provides some appropriate environment for excited state proton transfer process, and we believe that glucose moiety of OBG has some definite role in this overall ESPT process.

Furthermore time-resolved anisotropy measurements are performed to elucidate valuable information regarding the surrounding environment of the drug. The rotational relaxation of EPT in buffer takes place in 120 ps timescale. However, the anisotropy decay profile in presence of micellar medium exhibits noteworthy changes in the rotational diffusion time (Figure 4). The anisotropy decay of EPT in OBG micelles exhibits bi-exponential feature with correlation time constants of 120 ps and 2.6 ns with an average value of ~970 ps. The 120 ps component is believed to be originated from free EPT molecules, whereas 2.6 ns component can be assigned to the micelle encapsulated drug molecules. The increase in the relaxation time from 120 ps to 2.6 ns confirms the encapsulation of drug in OBG micelles, where EPT experiences more restricted environment compared to buffer medium. This further suggests that rigidity also have some role in the ESPT process of the drug in the excited state. The τ_r value is used to determine the hydrodynamic volumes from the Stokes–Einstein relationship;[50]

$$\tau_r = \frac{1}{6D_r} = \frac{\eta V}{kT}$$

Where D_r and η are the rotational diffusion coefficient and viscosity of the medium, respectively; V is the hydrodynamic molecular volume of the complex; and T is the absolute temperature. By using above equation and assuming that the viscosity of the medium is the same as that of water, the evaluated effective hydrodynamic diameter of the micelle is 28.09 Å. This value is in good agreement with the reported hydrodynamic diameter.[51]

Next we focus on the mechanism of excited state proton transfer in OBG micellar environment based on all the experimental evidences. Absorption data indicates the formation of ground state neutral EPT molecules after CMC of OBG, whereas steady state emission results infer the presence of both neutral and protonated species in OBG micellar environment. Excitation spectra monitored at 440 nm and 530 nm confirm that protonated species are formed exclusively in the excited state due to excited state proton transfer (Figure S2, Note S1) process. Moreover, the lifetime results suggest the existence of both neutral and protonated species in the excited state, and the protonated species formed at the cost of neutral one in ~4 ns time-scale. Time-resolved anisotropy results depict that the drug experiences restricted environment in OBG micelle. Interestingly, this kind of excited state proton transfer dynamics is not observed in other conventional micellar environments like SDS, CTAB and TX-100. In case of anionic SDS micelles, EPT exhibits protonated peak at 530 nm, whereas in CTAB and TX-100 micelles it shows emission from neutral form at 440 nm. These results can be explained by the interplay of two effects. The first one is the local dielectric constant felt by the EPT, and the second is the local proton concentration at the micellar surface. It is known that the local dielectric constant for all these three micellar systems is around 35-40.[52] Certainly, this environment doesn't favor charged species such as protonated form of EPT, and therefore, neutral form of EPT should be the stable species in all these micellar systems. The absorption and fluorescence spectra of TPT in TX-100 and CTAB micelles support this conjecture. Contrastingly, in SDS system the emission is

observed from protonated form instead of neutral form of the drug. This observation can be explained by the negative micellar surface attracting protons and making the local interfacial proton concentration much higher than the bulk solution of pH 7.[53,54] The presence of a higher proton concentration around SDS micelles appears to favor the protonation of the excited EPT under the local environment conditions and to compensate for the low polarity. Interestingly, unlike the other micellar systems, in excited state both neutral and protonated forms are observed in OBG micelles. Based on these observations we envisage that presence of glucose moiety and polarity of confined environment in OBG micelle take part major role for the conversion of neutral to protonated one in the excited state. It is already reported that the glucose molecules at first hydration shell of OBG micellar surface are projected inwards (away from bulk water) in the direction of the micellar hydrocarbon core, where the contact with water molecules is minimum.[55] Therefore, we anticipate that the drug molecules trapped in between the surfactants reside close to hydroxyl groups of glucose molecules, and thereby, excited state intermolecular proton transfer reaction takes place from glucose to drug molecules to yield excited state cationic form of the drug (Scheme 2). Local dielectric constant experienced by the drug molecule also contributes to the anomalous results obtained in OBG micelle. Though OBG micelles are neutral, the dielectric constant (~50)[56] at the palisade layer of OBG micelle is higher than that of above mentioned three micelles due to the presence of plenty of –OH groups at the interface of OBG micelle. Therefore, the higher local dielectric constant sensed by EPT molecule at the OBG micellar surface is also responsible for the stabilization charged species, such as protonated form of EPT in OBG micelle.

Our results suggest that EPT becomes less toxic in presence of OBG micellar environment, as absorption and emission results indicate the solubility of the drug increases in presence of OBG micellar environment. The drug loading to OBG micellar environment

can be easily monitored with the help of fluorescence switching from green to cyan color. Thus, considering biocompatible nature of OBG and above mentioned points, we believe that OBG micelle may act as a suitable drug delivery carrier for EPT. Most importantly, for the first time we have shown that the ESPT dynamics of ellipticine depends on both the polarity as well as surrounding proton concentration. Another important implication of our work is that one can predict cellular environment with respect to polarity as well as proton concentration from the ESPT process of the drug.

Conclusion

In the present work, we have studied the photophysical and proton transfer dynamics of an eminent anticancer drug, ellipticine inside a biocompatible octyl-β-D-glucoside (OBG) micellar medium using steady state as well as time resolved spectroscopic techniques. UV-visible absorption study reveals the conversion of protonated to neutral form of EPT, when OBG concentration reaches above critical micellar concentration. Interestingly, the emission at 530 nm (attributed to the protonated form of the drug) is also observed along with neutral form (emits at 440 nm), even when we selectively excite the neutral molecules. The above observation clearly demonstrates that excited state proton transfer process inside the OBG micelle is responsible for the conversion of neutral to protonated form of the drug. Time resolved emission measurements depict a pronounced enhancement in the average lifetime of both neutral and protonated species collected at 440 nm and 530 nm, respectively, when EPT is encapsulated inside OBG micelles. Astonishingly, a rise component of ~4 ns is observed in the time-resolved emission decays collected at 530 nm above CMC of OBG, and it is attributed to the excited state proton transfer dynamics of EPT inside OBG micellar confinement. Time-resolved area normalized emission spectra confirm the existence of two species in the excited state, where neutral form transforms to the protonated form. This kind

of proton transfer dynamics is absent in conventional micelles, like SDS, Triton X and CTAB, and therefore, indicates that the glucose molecules residing in the palisade layer of OBG micelle may have some role in the excited state proton transfer. Based on all the above observations, we conclude that the observed ESPT dynamics is a combined effect of local dielectric constant as well as presence of glucose moieties at the palisade layer of the OBG micelle.

Acknowledgement

PH is thankful to CSIR (Scheme no. 37(1499)/11/EMR-II) for financial support. RKK is thankful to University Grants Commission (UGC) for Junior Research Fellowship (JRF) and AS is thankful to CSIR for Senior Research Fellowship (SRF). Authors are indebted to Director, IISER-Pune for providing excellent experimental facilities. Authors thank to referees for their valuable comments and suggestions.

Supporting Information Available: This information is available free of charge via the internet at http://pubs.acs.org.

Reference

1. H. Luders, In Nonionic Surfactants: Alkylpolyglucosides; D. Balzer, H. Luders, Eds.; Dekker: NewYork, **2000**.
2. K. Holmberg, B. Jönsson, B. Kronberg and B. Lindman, Surfactants and Polymers in Aqueous Solution, 2nd ed.; Wiley: NewYork, **2002**; Chapter1.
3. L. Stryer, Biochemistry, 3rd ed.; W. H. Freeman and Company: New York, **1988**.
4. M. Kasahara and P. C. Hinkle, *Proc. Natl. Acad. Sci. U.S.A.*, 1976, **73**, 396-400.
5. M. Ollivon, O. Eidelman, R. Blumenthal and A. Walter, *Biochemistry*, 1988, **27**, 1695-1703.
6. P. K. Vinson, Y. Talmon and A. Walter, *Biophys. J.*, 1989, **56**, 669-681.
7. N. A. Dencher and M. P. Heyn, *FEBS Lett.*, 1978, **96**, 322-326.
8. H. Michel and D. Oesterhelt, *Proc. Natl. Acad. Sci. U.S.A.*, 1980, **77**, 1283-1285.
9. E. Fischer, *Ber. Dtsch. Chem. Ges.*, 1893, **26**, 2400-2412.
10. B. J. Boyd, C. J. Drummond, I. Krodkiewska and F. Grieser, *Langmuir*, 2000, **16**, 7359-7367.
11. F. Nilsson, O. Söderman and I. Johansson, *Langmuir*, 1996, **12**, 902-908.
12. D. Hantzschel, J. Schulte, S. Enders and K. Quitzsch, *Phys. Chem. Chem. Phys.*, 1999, **1**, 895-904.
13. H. D. Dörfler and A. Göpfert, *J. Disper. Sci. Technol.*, 1999, **20**, 35-58.
14. M. G. Bonicelli, G. F. Ceccaroni and C. La Mesa, *Colloid Polym. Sci.*, 1998, **276**, 109-116.
15. P. Sakya, J. M. Seddon and R. H. Templer, *J. Phys. II*, 1994, **4**, 1311-1331.
16. A. Loewenstein and D. Igner, *Liq. Cryst.*, 1991, **10**, 457-466.
17. V. Kocherbitov, O. Söderman and L. Wadsö, *J. Phys. Chem. B*, 2002, **106**, 2910-2917.
18. S. Ogawa, K. Asakura and S. Osanai, *Carbohydr. Res.*, 2010, **345**, 2534-2541.
19. K. K. Karukstis, W. C. Duim, G. R. Van Hecke and N. Hara, *J. Phys. Chem. B*, 2012, **116**, 3816-3822.
20. S. Ogawa, K. Asakura and S. Osanai, *Phys. Chem. Chem. Phys.*, 2012, **14**, 16312-16320.
21. M. V. C. Cardoso and E. Sabadini, *Langmuir*, 2013, **29**, 15778-15786.

22. S. Goodwin, A. F. Smith and E. C. Horning, *J. Am. Chem. Soc.*, 1959, **81**, 1903-1908.
23. J.-B. Le Pecq, X. Nguyen Dat, C. Gosse and C. Paoletti, *Proc. Natl. Acad. Sci. U.S.A.*, 1974, **71**, 5078-5082.
24. M. Ohashi and T. Oki, *Expert Opin. Ther. Pat.*, 1996, **6**, 1285-1294.
25. C. L. Arteaga, D. L. Kisner, A. Goodman and D. D. Von Hoff, *Eur. J. Cancer Clin. Oncol.*, 1987, **23**, 1621-1626.
26. F. Sureau, F. Moreau, J. M. Millot, M. Manfait, B. Allard, J. Aubard and M. A. Schwaller, *Biophys. J.*, 1993, **65**, 1767-1774.
27. S. Y. Fung, J. Duhamel and P. Chen, *J. Phys. Chem. A*, 2006, **110**, 11446-11454.
28. Z. Miskolczy, L. Biczók and I. Jablonkai, *Chem. Phys. Lett.*, 2006, **427**, 76-81.
29. S. Banerjee, A. Pabbathi, M. C. Sekhar and A. Samanta, *J. Phys. Chem. A*, 2011, **115**, 9217-9225.
30. K. Gavvala, A. Sengupta, R. K. Koninti and P. Hazra, *J. Phys. Chem. B*, 2013, **117**, 14099-14107.
31. M. Sbai, S. Ait Lyazidi, D. A. Lerner, B. del Castillo and M. A. Martin, *J. Pharm. Biomed. Anal.*, 1996, **14**, 959-965.
32. R. Thakur, A. Das and A. Chakraborty, *Chem. Phys. Lett.*, 2013, **563**, 37-42.
33. R. Thakur, A. Das and A. Chakraborty, *Phys. Chem. Chem. Phys.*, 2012, **14**, 15369-15378.
34. S. Y. Fung, H. Yang and P. Chen, *Colloids Surf., B*, 2007, **55**, 200-211.
35. S. Y. Fung, H. Yang, P. T. Bhola, P. Sadatmousavi, E. Muzar, M. Liu and P. Chen, *Adv. Funct. Mater.*, 2009, **19**, 74-83.
36. F. Zsila, J. Kaman, B. Boganyi and D. Jozsvai, *Org. Biomol. Chem.*, 2011, **9**, 4127-4137.
37. K. Gavvala, W. D. Sasikala, A. Sengupta, S. A. Dalvi, A. Mukherjee and P. Hazra, *Phys. Chem. Chem. Phys.*, 2013, **15**, 330-340.
38. K. Gavvala, R. K. Koninti, A. Sengupta and P. Hazra, *Phys. Chem. Chem. Phys.*, 2014, **16**, 2823-2826.
39. A. Sengupta, R. K. Koninti, K. Gavvala, N. Ballav and P. Hazra, *Phys. Chem. Chem. Phys.*, 2014, **16**, 3914-3917.
40. R. K. Koninti, A. Sengupta, K. Gavvala, N. Ballav and P. Hazra, *Nanoscale*, 2014, **6**, 2937-2944.
41. D. Mańko, A. Zdziennicka and B. Jańczuk, *Colloids Surf., B*, 2014, **114**, 170-176.

42. J. R. Lakowicz, 2006.
43. A. S. R. Koti, M. M. G. Krishna and N. Periasamy, *J. Phys. Chem. A*, 2001, **105**, 1767-1771.
44. A. S. R. Koti and N. Periasamy, *J. Chem. Phys.*, 2001, **115**, 7094-7099.
45. N. Sarker, K. Das, S. Das, A. Datta, D. Nath and K. Bhattacharyya, *J. Phys. Chem.*, 1995, **99**, 17711-17714.
46. P. K. Chowdhury, K. Das, A. Datta, W. Z. Liu, H. Y. Zhang and J. W. Petrich, *J. Photochem. Photobiol., A*, 2002, **154**, 107-116.
47. B. Cohen, D. Huppert, K. M. Solntsev, Y. Tsfadia, E. Nachliel and M. Gutman, *J. Am. Chem. Soc.*, 2002, **124**, 7539-7547.
48. A. S. Klymchenko, G. Duportail, Y. Mély and A. P. Demchenko, *Proc. Natl. Acad. Sci. U.S.A.*, 2003, **100**, 11219-11224.
49. T. K. Mukherjee, P. Ahuja, A. L. Koner and A. Datta, *J. Phys. Chem. B*, 2005, **109**, 12567-12573.
50. G. R. Fleming, Chemical Applications of Ultrafast Spectroscopy, Oxford, New York, **1986**.
51. B. Lorber, J. B. Bishop and L. J. DeLucas, *Biochim. Biophys. Acta, Biomembr.*, 1990, **1023**, 254-265.
52. F. Grieser and C. J. Drummond, *J. Phys. Chem.*, 1988, **92**, 5580-5593.
53. M. S. Fernandez and P. Fromherz, *J. Phys. Chem.*, 1977, **81**, 1755-1761.
54. B. Lovelock, F. Grieser and T. W. Healy, *J. Phys. Chem.*, 1985, **89**, 501-507.
55. P. Konidala, L. He and B. Niemeyer, *J. Mol. Graph. Model.*, 2006, **25**, 77-86.
56. C. J. Drummond, F. Grieser and T. W. Healy, *J. Chem. Soc., Faraday Trans. 1*, 1989, **85**, 551-560.

Table 1a. Fluorescence decay parameters of ellipticine in presence of OBG (0 to 100 mM) collected at 530 nm (λ_{ex} = 375 nm).

Concentration of OBG	τ_1(ns)	τ_2(ns)	τ_3(ns)	a_1	a_2	a_3	χ^2	τ_{avg} [#](ns)
Buffer	1.93	5.93	-	0.87	0.13	-	1.02	2.45
10 mM	2.03	5.61	-	0.85	0.15	-	1.02	2.57
17 mM	2.08	5.32	-	0.81	0.19	-	1.06	2.70
19 mM	2.25	6.13	-	0.83	0.17	-	1.03	2.91
23 mM	2.29	6.85	-	0.82	0.18	-	1.08	3.11
25 mM	2.30	9.76	-	0.62	0.38	-	1.02	5.13
26 mM	1.88	10.47	-	0.31	0.69	-	1.03	7.80
27 mM	-	10.77	4.33	-	1.16	-0.16	1.05	11.80
30 mM	-	11.52	3.79	-	1.89	-0.89	1.05	18.40
50 mM	-	12.27	3.82	-	2.17	-1.17	1.10	21.63
100 mM	-	12.82	4.27	-	2.17	-1.17	1.05	22.82

[#] $\tau_{avg} = a_1\tau_1 + a_2\tau_2$

Table 1b. Fluorescence decay parameters of ellipticine in presence of OBG (0 to 100 mM) collected at 440 nm (λ_{ex} = 375 nm).

Concentration of OBG	τ_1 (ns)	τ_2(ns)	τ_3(ns)	a_1	a_2	a_3	χ^2	τ_{avg} [#](ns)
Buffer	0.04	0.29	2.27	0.61	0.38	0.01	1.11	0.16
10 mM	0.05	0.33	3.56	0.66	0.32	0.02	1.12	0.21
17 mM	0.05	0.36	3.80	0.68	0.30	0.02	1.08	0.22
19 mM	0.05	0.38	4.02	0.63	0.34	0.03	1.05	0.28
23 mM	0.09	0.62	4.33	0.52	0.29	0.19	1.03	1.05
25 mM	0.25	1.93	4.21	0.35	0.29	0.37	1.05	2.20
26 mM	-	1.46	4.39	-	0.35	0.65	1.07	3.36
27 mM	-	1.77	4.27	-	0.35	0.65	1.05	3.40
30 mM	-	2.02	4.37	-	0.34	0.66	1.06	3.57
50 mM	-	2.19	4.27	-	0.31	0.69	1.01	3.62
100 mM	-	2.01	4.23	-	0.30	0.70	1.04	3.56

[#] $\tau_{avg} = a_1\tau_1 + a_2\tau_2$

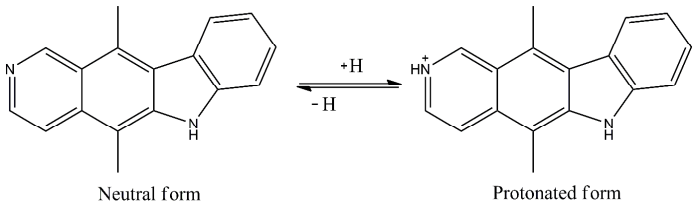

Scheme 1. Different prototropic forms of ellipticine.

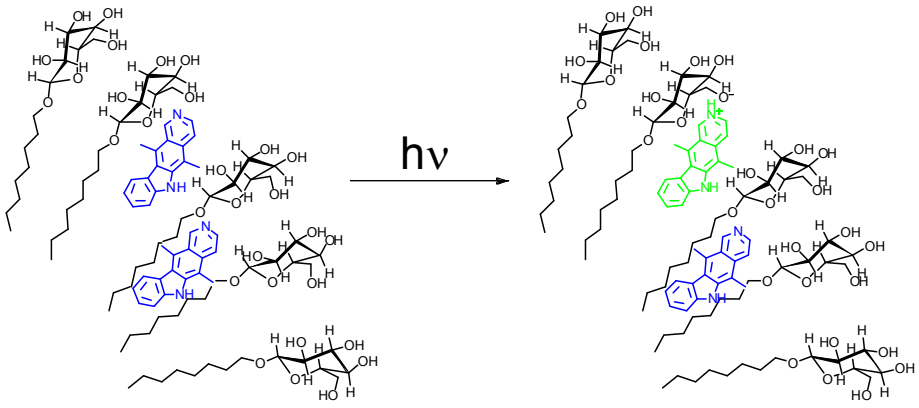

Scheme 2. Excited state proton transfer process of EPT in octyl-β-D-glucoside micelle.

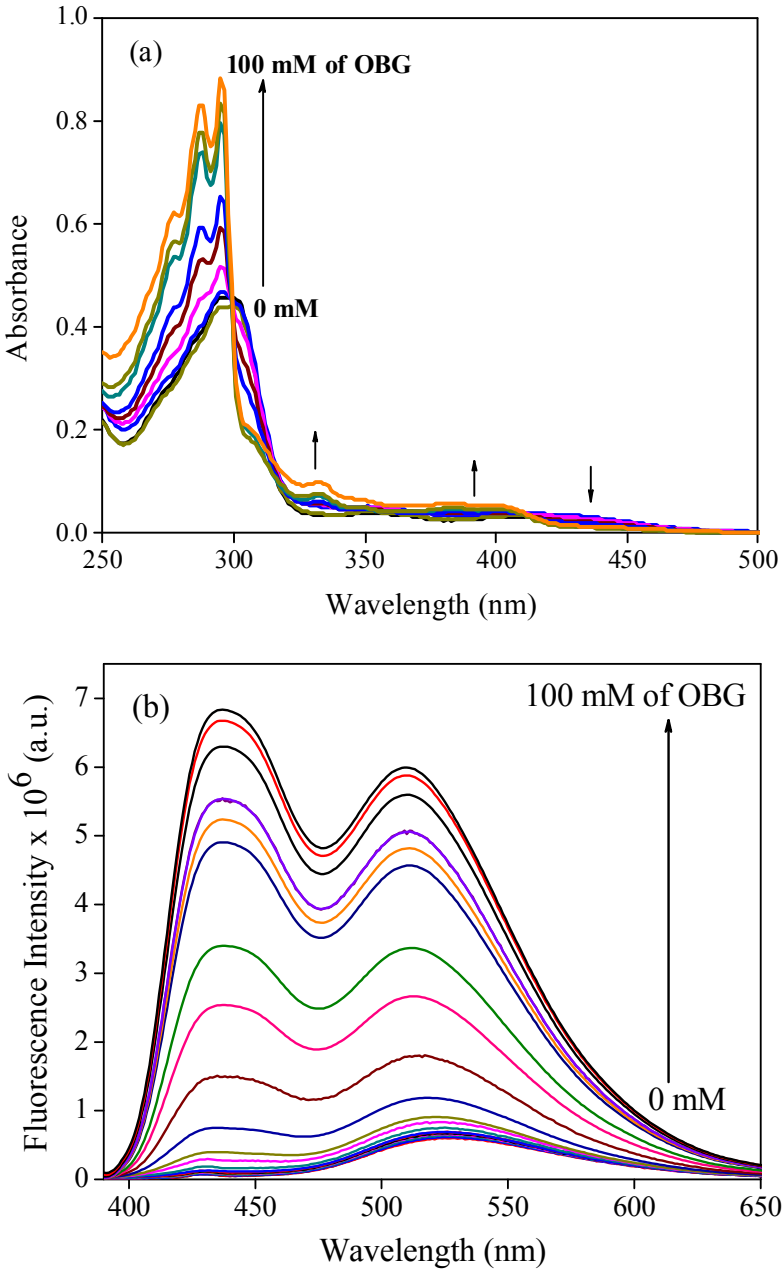

Figure 1. Absorption (a) and Emission (λ_{ex} = 375 nm) (b) spectra of EPT in pH 7 buffer with increasing concentration of OBG (0 mM to 100 mM).

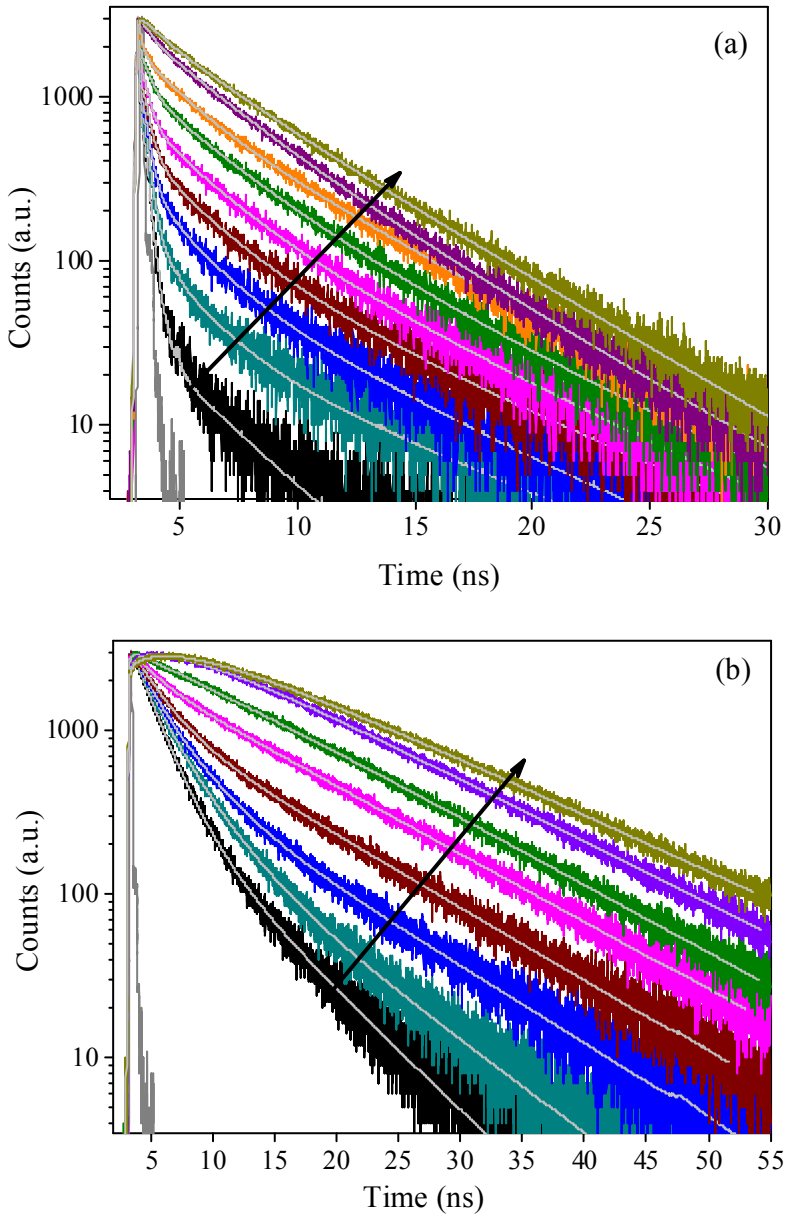

Figure 2. Time resolved fluorescence decays of EPT in pH 7 buffer with increasing concentration of OBG (0 mM to 100 mM) collected at 440 nm (a) and 530 nm (b) (λ_{ex} = 375 nm).

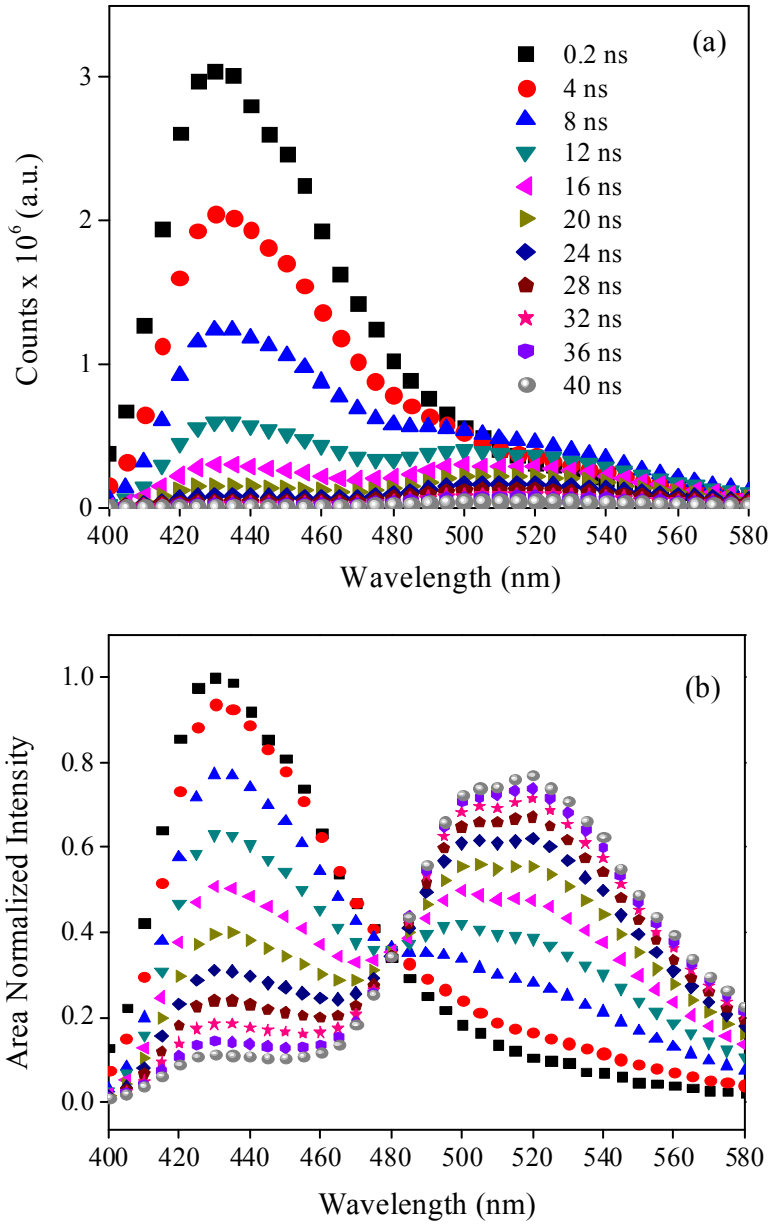

Figure 3. (a) Time resolved emission spectra (TRES) and (b) time resolved area normalized emission spectra (TRANES) of EPT in presence of 100 mM of OBG.

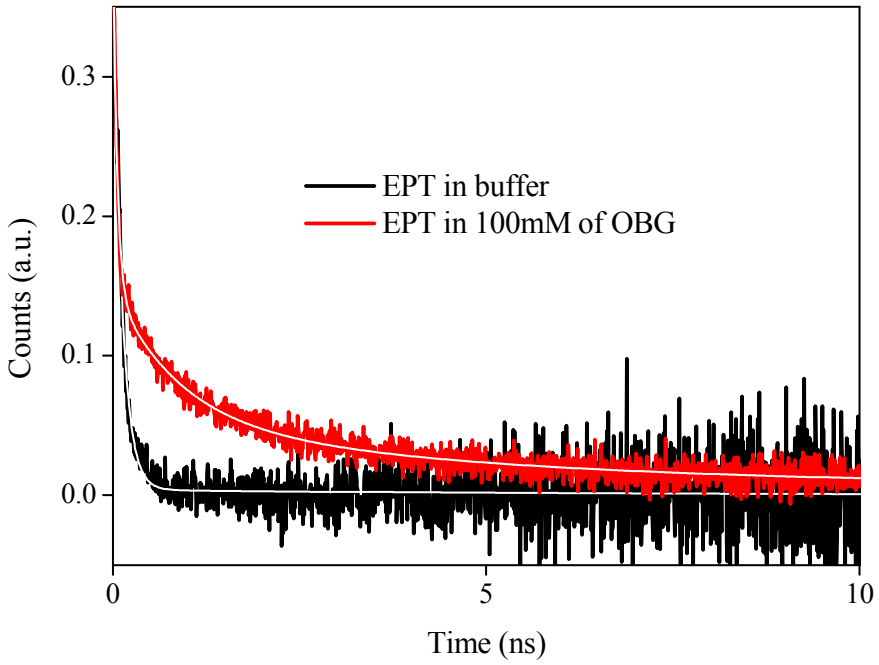

Figure 4. Time resolved anisotropy decays of EPT in pH 7 buffer collected at 530 nm and in presence of 100 mM of OBG collected at 440 nm in emission spectrum (λ_{ex} = 375 nm).